

**National Oceanography Centre, Southampton**

**Research & Consultancy Report No. 50**

Coupling the PLANKTOM5.0 marine ecosystem model to the  
OCCAM I° ocean general circulation model for investigation  
of the sensitivity of global biogeochemical cycles to variations  
in ecosystem complexity and physical environment

B Sinha & T R Anderson

2008

National Oceanography Centre, Southampton  
University of Southampton, Waterfront Campus  
European Way  
Southampton  
Hants SO14 3ZH UK

Author contact details:  
Tel: +44 (0)23 8059 7742  
Email: [bs@noc.soton.ac.uk](mailto:bs@noc.soton.ac.uk)

## *DOCUMENT DATA SHEET*

<i>AUTHOR</i> SINHA, B & ANDERSON, T R	<i>PUBLICATION DATE</i> 2008
<i>TITLE</i> Coupling the PLANKTOM5.0 marine ecosystem model to the OCCAM 1° ocean general circulation model for investigation of the sensitivity of global biogeochemical cycles to variations in ecosystem complexity and physical environment.	
<i>REFERENCE</i> Southampton, UK: National Oceanography Centre, Southampton, 36pp. (National Oceanography Centre Southampton Research and Consultancy Report, No. 50) (Unpublished manuscript)	
<i>ABSTRACT</i> <p>The earliest marine ecosystem models consisted of a simple representation of the main features of marine ecosystems, including, typically, variables for phytoplankton, zooplankton, nutrient and detritus (NPZD models). These have been incorporated into ocean general circulation models to give a basic representation of ecosystem function, providing predictions of bulk quantities such as global primary production, export and biomass which can be compared with available observations. A recent trend has been to increase the number of phytoplankton and zooplankton groups modelled, as analogues of different plankton groups observed to exist in the ocean, for example diatoms and coccolithophores (the so-called plankton functional type or PFT approach). It is usually assumed that the increase in complexity of the model will result in simulated ecosystems which more faithfully reproduce observations than NPZD models, but this has not been demonstrated systematically. The robustness of the PFT models to changes in model parameters and to changes to the physical environment in which it is embedded, have not been investigated. As a first step towards these goals, we incorporate a state-of-the-art PFT model, PLANKTOM5.0 into the OCCAM ocean general circulation model. A 6 year simulation is performed, covering the years 1989-1994 with identical parameter choices to an existing run of PLANKTOM5.0 coupled to the OPA general circulation model. This document describes the development of the coupled model and the 6 year simulation. Comparison with the OPA model and sensitivity of the solution to parameter choices will be described in a forthcoming journal paper.</p>	
<i>KEYWORDS</i>  biogeochemical cycles, global domain, model complexity, Plankton ecosystem, physical model	
<i>ISSUING ORGANISATION</i> <b>National Oceanography Centre, Southampton University of Southampton, Waterfront Campus European Way Southampton SO14 3ZH UK</b>	
<i>Not generally distributed - please refer to author</i>	

## **Contents**

Abstract	6
1. Overview	7
2. 1° OCCAM GCM adapted for biology and carbon biogeochemistry	7
3. The PLANKTOM5.0 marine biogeochemical model	9
3.1 Photic Zone	11
3.2 Aphotic zone	18
3.3 Parameterizations of transfer processes	21
3.4 Changes introduced to the PLANKTOM5.0 code	25
4. Experimental set up and input files	29
5. Results	32
6. Acknowledgements	35
7. References	35

## List of Figures

- 1 (a) Diagrammatic representation of the model phosphorus cycle in the photic zone, showing pathways and processes transferring material between Dissolved Inorganic Phosphate ( $\text{PO}_4$ ), Dissolved Organic Phosphate (DOP), Phytoplankton (P), Zooplankton (Z) and Detritus (D) pools. (b) Similar diagram for the model carbon cycle (DIC = dissolved inorganic carbon, DOC = Dissolved Organic Carbon). 11
- 2 More detailed view of the model phosphorus and carbon cycles in the photic zone. POC = small particulates, GOC = large particulates, mix = mixed phytoplankton, dia = diatoms, coc = coccolithophores, micro = microzooplankton, meso = mesozooplankton. 12
- 3 Diagrammatic representation of the model silicate cycle in the photic zone, showing pathways and processes transferring material between Dissolved Silicate (Si), Particulate Silica (DSi), and Biogenic Silica (BSi). 13
- 4 Diagrammatic representation of the model iron cycle in the photic zone, showing pathways and processes transferring material between Dissolved Iron (Fe), Phytoplankton (P), Zooplankton (Z) and Detritus (D) pools. 14
- 5 More detailed view of the model iron cycle in the photic zone. SFe = small particulates, BFe = large particulates, mix = mixed phytoplankton, dia = diatoms, coc = coccolithophores, micro = microzooplankton, meso = mesozooplankton. 15
- 6 Production and destruction of model chlorophyll in the photic zone. 16
- 7 (a) Diagrammatic representation of the model calcite cycle in the photic zone, showing pathways and processes transferring material between Dissolved Inorganic Carbon (DIC), calcite attached to coccolithophores, and detached coccoliths (b) Similar diagram for the model alkalinity (ALK) (c) changes in alkalinity due to production, remineralization and zooplankton respiration. 17
- 8 Production and consumption of model oxygen in the photic zone. 17
- 9 (a) Diagrammatic representation of the model phosphorus cycle in the aphotic zone (b) Similar diagram for the model carbon cycle. 18
- 10 More detailed view of the model phosphorus and carbon cycles in the aphotic zone. 18
- 11 Diagrammatic representation of model silicate cycle in the aphotic zone. 19
- 12 (a) Diagrammatic representation of the model iron cycle in the aphotic zone (b) more detailed view. 19
- 13 Diagrammatic representation of model chlorophyll in the aphotic zone. 20
- 14 Diagrammatic representation of model calcite/alkalinity cycles in the aphotic zone. 20

15 Diagrammatic representation of model oxygen in the aphotic zone.	21
16 Monthly mean dust input files ( $\text{g m}^{-2} \text{ month}^{-1}$ ) (a) January (b) July.	30
17 Annual mean river input files ( $\text{Tg yr}^{-1}$ per model box) (a) DIC, OCCAM grid 1 (b) DIC, OCCAM grid 2 (b) DOC, OCCAM grid 1 (c) DOC, OCCAM grid2. Axes labels denote model gridpoint indices.	31
18 Annual mean surface fields from year 1994 of the PLANKTOM-OCCAM simulation (a) mixed phytoplankton (b) diatoms (c) coccolithophores (d) microzooplankton (e) mesozooplankton (f) phosphate (g) silicate (h) iron (i) POC. Plankton fields and POC are in $\text{mmol C m}^{-3}$ . Phosphate is in $\text{mmol PO}_4 \text{ m}^{-3}$ , Silicate is in $\text{mmol SiO}_3 \text{ m}^{-3}$ , iron is in $\mu\text{mol Fe m}^{-3}$ .	32
19 Annual mean surface fields from year 1994 of the PLANKTOM-OCCAM simulation (a) GOC in $\text{mmol C m}^{-3}$ (b) sea-surface temperature in $^{\circ}\text{C}$ (c) mean daily maximum mixed layer depth in m (d) alkalinity in $\text{mmol m}^{-3}$ (e) oxygen in $\text{mmol m}^{-3}$ (f) calcite in $\text{mmol m}^{-3}$ (g) DOC in $\text{mmol C m}^{-3}$ (h) DIC in $\text{mmol C m}^{-3}$ (i) SFE in $\text{nmol Fe m}^{-3}$ .	33
20 Annual mean surface fields from year 1994 of the PLANKTOM-OCCAM simulation (a) BFE (b) DSI (c) DFE (d) NFE (e) CFE (f) DCH (g) NCH (h) CCH. Iron fields are in $\text{nmol Fe m}^{-3}$ . Chlorophyll fields are in $\text{mg m}^{-3}$ . DSI is in $\text{mmol m}^{-3}$ .	34

## **List of Tables**

1 List of biogeochemical tracers in PLANKTOM5.0 and abbreviations used.	10
---	----

## **Abstract**

The earliest marine ecosystem models consisted of a simple representation of the main features of marine ecosystems, including, typically, variables for phytoplankton, zooplankton, nutrient and detritus (NPZD models). These have been incorporated into ocean general circulation models to give a basic representation of ecosystem function, providing predictions of bulk quantities such as global primary production, export and biomass which can be compared with available observations. A recent trend has been to increase the number of phytoplankton and zooplankton groups modelled, as analogues of different plankton groups observed to exist in the ocean, for example diatoms and coccolithophores (the so-called plankton functional type or PFT approach). It is usually assumed that the increase in complexity of the model will result in simulated ecosystems which more faithfully reproduce observations than NPZD models, but this has not been demonstrated systematically. The robustness of the PFT models to changes in model parameters and to changes to the physical environment in which it is embedded, have not been investigated. As a first step towards these goals, we incorporate a state-of-the-art PFT model, PLANKTOM5.0 into the OCCAM ocean general circulation model. A 6 year simulation is performed, covering the years 1989-1994 with identical parameter choices to an existing run of PLANKTOM5.0 coupled to the OPA general circulation model. This document describes the development of the coupled model and the 6 year simulation. Comparison with the OPA model and sensitivity of the solution to parameter choices will be described in a forthcoming journal paper.

## 1. Overview

This document is an account of a medium resolution (1° horizontal resolution) coupled ocean-biology-biogeochemistry climate model, with a relatively complex representation of the ecosystem (3 phytoplankton and 2 zooplankton types).

It consists of a physical ocean General Circulation Model (GCM), OCCAM (Ocean Circulation and Climate Advanced Modelling project, see Coward and de Cuevas for a technical description of the ¼° version of OCCAM and Marsh et al., 2004, 2005 for analysis of results) coupled to a biogeochemical model, PLANKTOM5.0 (Le Quere et al., 2005). The method employed in coupling is basically the same as for previous biological/biogeochemical models based on OCCAM, OB1 (Popova et al, 2006a,b), and ONOC1 (Sinha and Yool, 2006, hereinafter SY06, and Yool and Sinha, 2006, hereinafter YS06). In particular the reader is advised to refer extensively to SY06, as much relevant material will not be repeated here.

The intention is to compare model predictions of bulk biological quantities (total phytoplankton biomass, total zooplankton biomass, primary production, export) with the equivalents from an NPZD model (Popova et al, 2006a,b) and with a separate simulation based on PLANKTOM5.0 coupled to the OPA physical model as well as with available observations. In addition we intend to compare ecosystem structure (e.g. biomass partitioned between diatoms, coccolithophores and mixed phytoplankton) between PLANKTOM-OCCAM and PLANKTOM-OPA.

Our ultimate aim is to evaluate the plankton functional type approach in terms of gains in realism compared with NPZD models, in terms of sensitivity to parameter choices, and in terms of sensitivity to choice of physical model.

The document itself is organized as follows: Section 2 gives a very brief overview of the 1° OCCAM general circulation model adapted for biology and carbon biogeochemistry as this is well documented elsewhere, and lists changes made specifically for incorporation of PLANKTOM5.0; Section 3 Describes the PLANKTOM5.0 marine ecosystem model in some detail and notes any changes made specifically for embedding in OCCAM; Section 4 describes the model experiment setup and input files; Section 5 describes the model results.

## 2. 1° OCCAM GCM adapted for biology and carbon biogeochemistry

This is extensively documented SY06 and YS06, and will not be repeated here. In particular the reader is recommended to refer to Part A, Section 5 (“OCCAM”, pp13-27), Section 6 (“Modifications to the ocean model”, pp28-33) and Section 7 (“Step-by-step procedure to compile and run the model”, pp34-37) of SY06. The main differences between the present OCCAM code and that of SY06 arise due to the following:

- 1 PLANKTOM5.0 requires 27 3D biogeochemical tracer fields compared to 10 for ONOC1



- 2 PLANKTOM5.0 needs to read in 12 monthly mean 2D fields for surface dust input (from which surface inputs of silicate and iron are derived) and 3 annual mean fields of riverine inputs of dissolved inorganic carbon (DIC), dissolved organic carbon (DOC) and the mask of coastal sea-points (cmask33). These are read in once at the start of a simulation. Surface inputs of silicate and iron are derived from dust input. Riverine input of silicate is derived from DIC, input of phosphate from DIC and DOC, and of iron from the coastal mask. Details of the input files and their derivation are given in Section 4.
- 3 PLANKTOM5.0 needs to read in daily 2D surface irradiance fields. These must be read in “on the fly” as required.
- 4 Global integrals of denitrification, potential nitrogen fixation, and dissolved silicate, particulate silicate and particulate carbon need to be calculated for use in the biogeochemical equations.
- 5 Globally integrated diagnostics of all the biogeochemical tendency terms are calculated during the model simulation.

The code changes required for these five items are listed in order below. The reader is requested to refer to Section 6 of SY06.

1 NT is changed to 29 (temperature, salinity and 27 biogeochemical tracers) in param.h

Each tracer is given a name and units in moddata.h

Fortran unit numbers are assigned for each tracer variable (see p29 of SY06).

2 fields.h is modified to include 2D tracer fields for dust and riverine input of dic, doc, and iron (rdust, rdic, rdoc and cmask33). A temporary array maxmld is also defined. caesar.F is modified to read in these files sequentially before the main timestepping loop and distribute the data to the individual processors via calls to m\_send.F. A new message code, MAXMLD, is used for these calls. m\_send.F is therefore modified to include this new type of message, and s\_recv.F is modified so the message can be received. Finally legion.F is modified to receive the distributed data before beginning the timestepping calculations.

3 A 2D array for surface irradiance (sw\_uea) is defined in cvbc.h. These fields must be read in each model day and then distributed to the processors, so the procedure is slightly different to item 2, where the same temporary arrays which are used to read in restarts (rest2d\_1 and rest2d\_2) were used to read in the dust and river fields. It was found necessary to define new temporary arrays in caesar.F (best2d\_1, and best2d\_2), and associated buffers, bestbuf\_1 and bestbuf\_2. metrd\_ncar.F was modified to open the irradiance files and to read the fields into best2d\_1 and best2d\_2 in addition to reading in the usual forcing for the OCCAM physical model (i.e. NCEP-derived winds, air temperature, humidity etc). After calling metrd\_ncar, caesar.F sends the forcing data to the individual processors via the m\_send routine, using message code MSG\_WIN3. m\_send.F therefore had to be modified to include dispatch of the new irradiance data to the individual processors. Similarly s\_recv.F had to be modified to receive the irradiance data from m\_send.F and place it in array swflux\_uea where it is available for use by the biogeochemical routines.

4 Implementation of the global integrals was quite tricky, but the model already performs something similar for the surface water flux correction, evap0, so this procedure was copied. The sequence is as follows: on starting a run, the global integral is initialized to zero or read in from the last restart file – archrd.F was modified to do this for the five extra global integrals required in addition to evap0 (these are named as dtot0, dtot20, dtot30, dtot40 and

dtot50, corresponding to denitrification, dissolved silicate, particulate silicate, particulate carbon and potential nitrogen fixation respectively). The model then sends the global integrals to the slave processors, via `m_send.F`, using message code `MSG_TIMEVAR`. `m_send.F` was therefore modified to send the extra global integrals and `s_recv.F` was modified to receive them. These global integrals are then available for use by the slave processors. The slave processors then calculate new integrals using the data available to them (i.e. each processor calculates an integral over its part of the global domain, this is performed in subroutine `bgcsed.F`). The new integrals are then sent back to the master via `s_send.F` using message code `MSG_RY_VOL`. `s_send.F` was therefore modified to send the new integrals (known as `ddtot`, `ddtot2`, `ddtot3`, `ddtot4` and `ddtot5`) and `m_recv.F` was modified to receive them and sum the values over all the processors, so obtaining a new global integral and completing the loop. Finally `archwr.F` was modified to output the extra global integrals to the grid 1 restart file so they are available if the model is restarted at any point.

It was also necessary to add an extra `#ifdef` option in the makefile called `dgom_start`. If a run is begun from a restart which does not contain the extra global integrals, the model needs to be compiled with this option, and it will initially set the extra integrals to zero and output them to any restart files it generates. If a run is to be begun from a restart which does contain the extra integrals, then it is necessary to compile without the `dgom_start` option in the makefile. In both cases, if changing the makefile, it is wisest to type “make clean” before recompiling the code to avoid possible conflicts.

5 scalar variables for tendency term diagnostics are declared in `cvbc.h`. A simple approach was adopted whereby each legion calculates the diagnostics over its own domain and outputs directly to its `lgnb` output file, thus avoiding the complications of item 4. The master is not involved so no new message passing is necessary. `step.F` is modified to initialise and output the sums. The terms themselves are calculated in `bgcbio.F` and are described in the next section. However it was found that the model could not cope with all the terms for phosphate, iron and silicate cycles in the same run, so as a compromise a `#ifdef` flag is used to decide which of the 3 nutrient cycles will be diagnosed – it is necessary to recompile the code with either `-Dpo4diags`, `-Dferdiags` or `-Dsildiags` in the makefile.

### **3. The PLANKTOM5.0 marine biogeochemical model**

This model is well documented on the Green Ocean website ([http://lgmaweb.env.uea.ac.uk/green\\_ocean](http://lgmaweb.env.uea.ac.uk/green_ocean)) and hence many details such as the model equations and choice of parameter values are not presented here. However it is necessary to go into a certain level of detail in order to explain how the model was modified to fit into the framework of the OCCAM model. Additionally, whilst it is easy to get a good overview of the model from the web based material, some aspects are not dealt with, in particular, diagrams of the modelled flows of material between the state variables such as are provided here.

The model includes three types of phytoplankton (diatoms or ‘silicifiers’, mixed phytoplankton and coccolithophores or ‘calcifiers’) and two types of zooplankton (mesozooplankton and microzooplankton). There are 3 nutrients (silicate, phosphate and iron). Only diatoms contain silicate whereas all three phytoplankton types contain phosphate, chlorophyll and iron. There are also two size classes of sinking detritus (particulate organic carbon) and one class of sinking particulate silica. Both types of particulate organic carbon

contain iron. Dissolved inorganic and organic carbon pools are included. Finally, calcite, oxygen and alkalinity cycles are treated. The surface (euphotic) zone has a fixed depth and is treated separately to the deeper ocean. A list of the biogeochemical tracers used in the model is presented in Table 1 along with 3-letter abbreviations used for each throughout this document.

variable	abbreviation	variable	abbreviation	variable	abbreviation
alkalinity	TAL	meso-zooplankton	MES	iron content of mixed phytoplankton	NFE
calcite	CAL	dissolved inorganic carbon	DIC	iron content of coccolithophores	CFE
dissolved organic carbon	DOC	dissolved iron	FER	chlorophyll content of diatoms	DCH
small particulates (carbon)	POC	dissolved silicate	SIL	chlorophyll content of mixed phytoplankton	NCH
large particulates (carbon)	GOC	dissolved inorganic phosphate	PO4	chlorophyll content of coccolithophores	CCH
small particulates (iron)	SFE	carbon content of diatoms	DIA	silicate content of diatoms	DSI
large particulates (iron)	BFE	carbon content of mixed zooplankton	MIX	dissolved oxygen	OXY
particulate silica	DSI	carbon content of coccolithophores	COC		
micro-zooplankton	MIC	iron content of diatoms	dfe		

Table 1 List of biogeochemical tracers in PLANKTOM5.0 and abbreviations used.

### 3.1 PHOTIC ZONE

#### Phosphate/carbon cycles

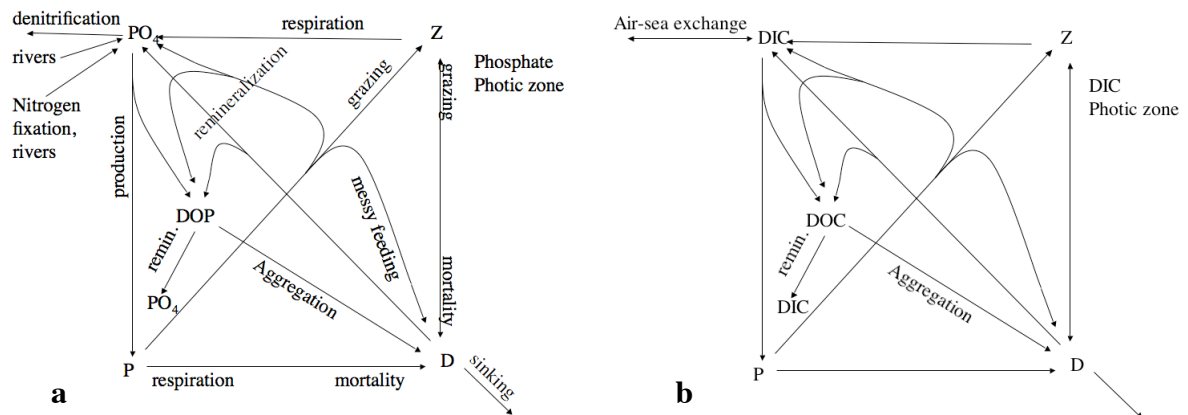


Figure 1. (a) Diagrammatic representation of the model phosphorus cycle in the photic zone, showing pathways and processes transferring material between Dissolved Inorganic Phosphate ( $PO_4$ ), Dissolved Organic Phosphate (DOP), Phytoplankton (P), Zooplankton (Z) and Detritus (D) pools (b) Similar diagram for the model carbon cycle (DIC = dissolved inorganic carbon, DOC = Dissolved Organic Carbon).

Fig. 1 shows the transfers of phosphorus (Fig. 1a) and carbon (Fig. 1b) between the various components: phytoplankton (P), zooplankton (Z), detritus (D), dissolved inorganic phosphate (DIP) and dissolved inorganic carbon (DIC). The diagrams are very similar since in the model the carbon:phosphate ratio is fixed in organic material (=1:122). However the ratio of inorganic C:P can vary depending on the amount of denitrification/nitrogen fixation which affects phosphate only, or air-sea exchange which affects DIC only. Hence the same equations (and tracers for P, Z, and D) are used for the C and P cycles, but different terms are added to the inorganic phases to represent the processes of denitrification/nitrogen fixation and air-sea exchange. DIP and DIC are therefore represented by separate tracers.

Phytoplankton produce organic material from DIP/DIC. The amount of production is limited by light and nutrient availability. A proportion is used to fuel phytoplankton growth, with the remainder entering the pool of dissolved organic phosphate (DOP) or carbon (DOC). Respiration and mortality transfer material from phytoplankton to detritus, which consists of particulate organic carbon/phosphate. Zooplankton feed on phytoplankton and detritus, with different preferences (preferences are described further in Section 3.3). The grazing process is somewhat complicated. A proportion of total grazing (“growth efficiency”) is used for zooplankton growth, another proportion is converted directly to detritus (“messy feeding”) and a further proportion is remineralized either directly to DIP/DIC, or to DOP/DOC. These pathways are shown in Fig. 1 for grazing on phytoplankton, but not for grazing on detritus to avoid overly complicating the Figure. Zooplankton respiration transfers material back to phosphate or DIC, whilst mortality of both phytoplankton and zooplankton transfers material to detritus. Detritus sinks down the water column, remineralizing as it does so. Remineralization converts detritus to DIP/DIC, with a proportion going to DOP/DOC.

Finally, DOP/DOC can remineralise phosphate or carbon back to the dissolved state, or aggregate to form detritus.

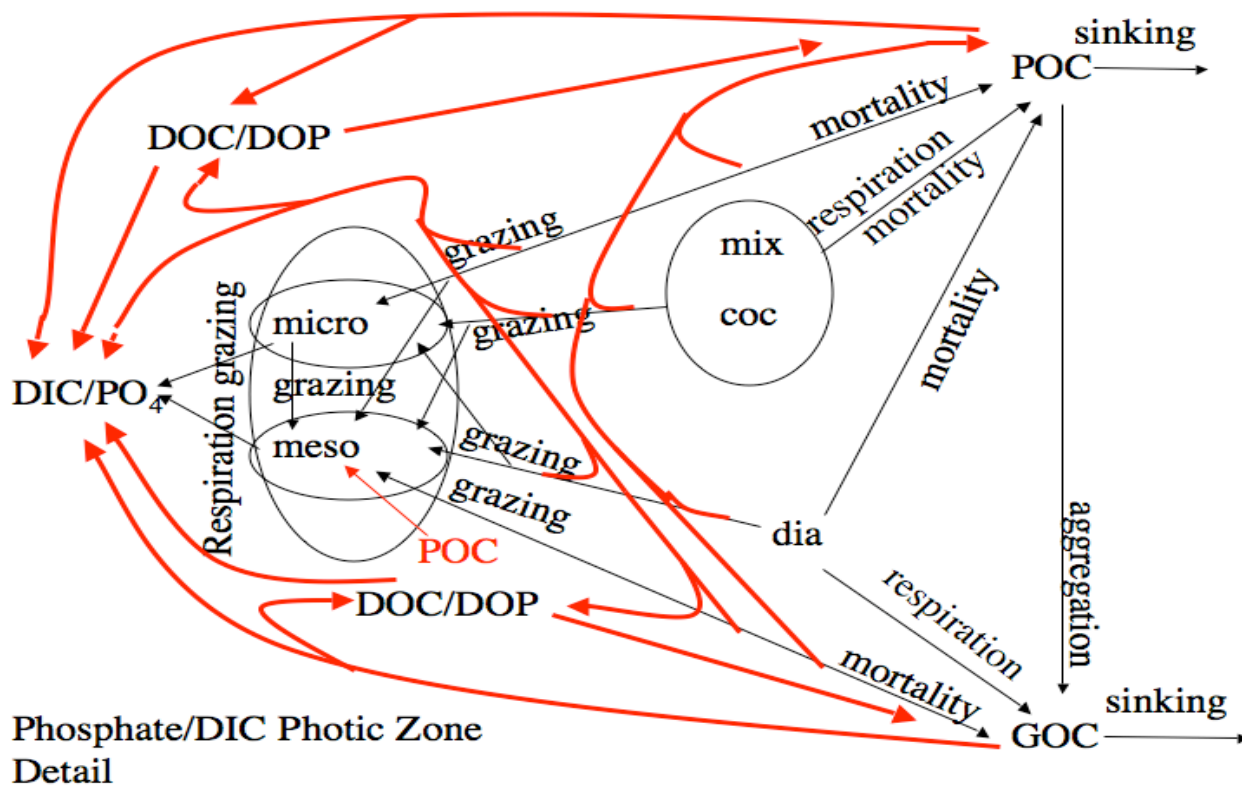


Figure 2. More detailed view of the model phosphorus and carbon cycles in the photic zone. POC = small particulates, GOC = large particulates, mix = mixed phytoplankton, dia = diatoms, coc = coccolithophores, micro = microzooplankton, meso = mesozooplankton.

There is an overall input of DIP to the system from rivers which is balanced by sedimentation of detritus at the ocean bottom (Figures 9a and 10 below). Note that the sedimentation of detritus removes carbon as well as phosphate from the system, although the riverine input of DIP does not input an equivalent amount of DIC. Thus the total amount of phosphate is conserved, but the total amount of carbon is not.

Three phytoplankton groups are represented: mixed phytoplankton (mix), diatoms (dia) and coccolithophores (coc) with different rates of production and mortality (Fig. 2, for clarity transfers due to production have been left out). Similarly two types of zooplankton (micro- and mesozooplankton) are included with different grazing preferences for the different types of phytoplankton and detritus (mesozooplankton can also graze on microzooplankton). Two types of detritus are included: small/slow-sinking (POC) and large/fast-sinking (GOC). Phytoplankton mortality transfers phosphate and carbon to POC independent of functional type. Microzooplankton mortality transfers material to POC (although the microzooplankton mortality rate is set to zero in the version considered here), whereas mesozooplankton

mortality transfers material to GOC. Respiration of mixed phytoplankton and coccolithophores transfers material to POC whereas respiration by diatoms transfers material to GOC. Respiration of both types of zooplankton results in transfer to inorganic phosphate and carbon. Material can also flow from POC to GOC via aggregation. Remineralization pathways, including those via DOP/DOC are shown as red arrows. Of the total carbon ingested by zooplankton, a variable proportion, called the grazing efficiency, is used for growth, a fixed proportion is recycled to POC (small detritus) and the remainder is converted to either dissolved DIP/DIC or DOP/DOC. The value of the grazing efficiency depends on the ratio of zooplankton respiration to total grazing and also on the average iron:phosphate ratio of the prey (see section on the iron cycle below).

### Silicate cycle

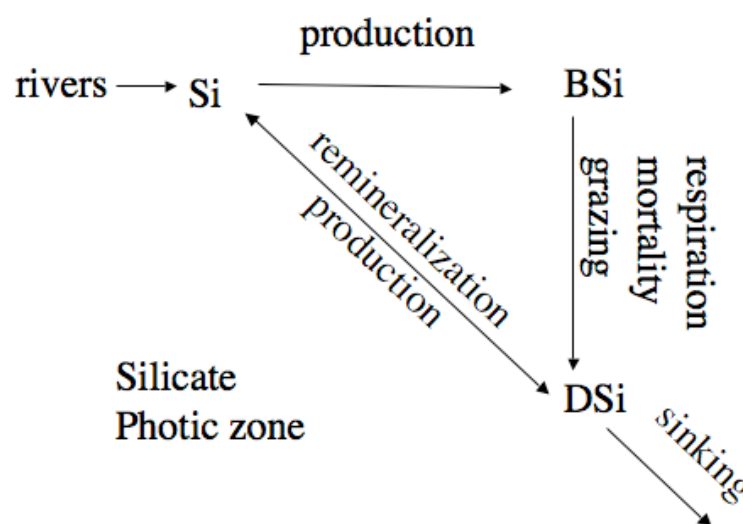


Figure 3. Diagrammatic representation of the model silicate cycle in the photic zone, showing pathways and processes transferring material between Dissolved Silicate (Si), Particulate Silica (DSi), and Biogenic Silica (BSi).

Diatoms require the addition of a silicate cycle (Fig. 3). Three further tracers are required: dissolved silicate, silicate incorporated in diatoms (BSi) and particulate (or 'detrital') silica (DSi). Zooplankton are assumed to contain no silicate, so grazing transfers silicate directly from diatoms to detritus.

Apart from sinking, remineralization and sedimentation, the transfer terms (i.e. production, respiration, mortality and grazing) are derived from the corresponding phosphate terms for diatoms, modified by the variable ratio of silicate to phosphate in the diatoms. A proportion of production is used to fuel incorporation of silicate into diatoms, whilst the remainder is converted to sinking silica. Input of silicate by dust and rivers at the surface is balanced by loss of silicate at the bottom box by sedimentation so that the total amount of silicate is conserved.

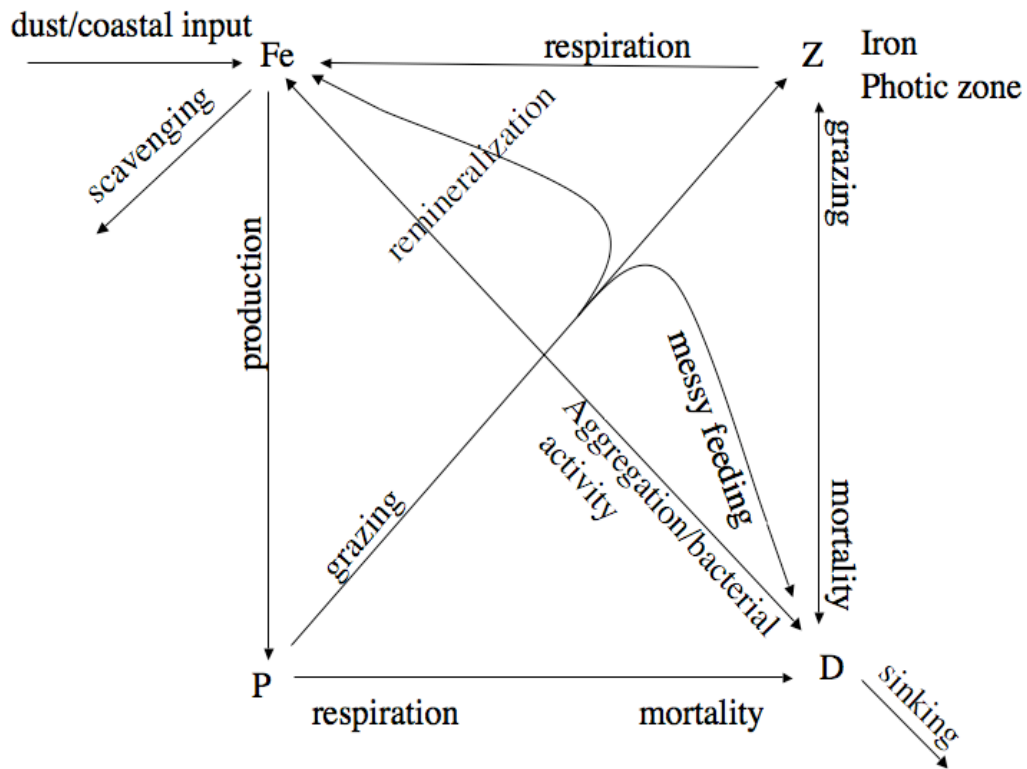


Figure 4. Diagrammatic representation of the model iron cycle in the photic zone, showing pathways and processes transferring material between Dissolved Iron (Fe), Phytoplankton (P), Zooplankton (Z) and Detritus (D) pools.

### Iron cycle

The iron cycle is somewhat similar to the phosphate and carbon cycles (Fig 4).

The iron content of the phytoplankton is explicitly modelled which means the iron:phosphate ratio can vary. Iron is taken up from the dissolved state at varying rates by all three phytoplankton types. Processes of respiration, and mortality transfer iron from phytoplankton to detritus which can remineralize back to dissolved iron, or sink. Zooplankton are assumed to have an Fe/PO<sub>4</sub> ratio of 5x10<sup>-6</sup>. The loss of iron from each phytoplankton type due to grazing by zooplankton is obtained from the appropriate terms for phosphate, multiplied by the ratio of iron:phosphate for that phytoplankton type (the transfer terms for respiration and mortality are obtained similarly). As with phosphate, a variable proportion of the total grazing is incorporated into zooplankton, a fixed proportion is recycled to (small) particulate iron and the remainder is transferred to dissolved iron. Of the proportion used to fuel phytoplankton growth, some cannot be incorporated into zooplankton because they have a fixed iron:phosphate ratio, so any excess iron is recycled back to dissolved iron. The opposite problem occurs if the prey do not have sufficient iron to make up the iron:phosphate ratio of zooplankton. Rather than take iron from the dissolved pool, the model alters the minimum

grazing efficiency so that less phosphate is taken up by the zooplankton. Of course when mesozooplankton graze on microzooplankton, this situation does not arise as both predator and prey have the same iron:phosphate ratio. Production for iron is computed from a slightly different formula to that for phosphate/carbon. Bacterial activity is parameterized and can lead to conversion of dissolved iron to particulates, as can aggregation. The other difference is that there is no pool of dissolved organic iron so the pathways are somewhat simpler. Iron can be input to the system by dust and coastal input and can be removed by scavenging. However there is no requirement for the total iron content to be conserved. There is no sedimentation at the bottom for iron. As with phosphate/carbon, the various plankton functional types have slightly different behaviour (Fig. 5), but the absence of a dissolved organic phase makes the exchanges easier to follow.

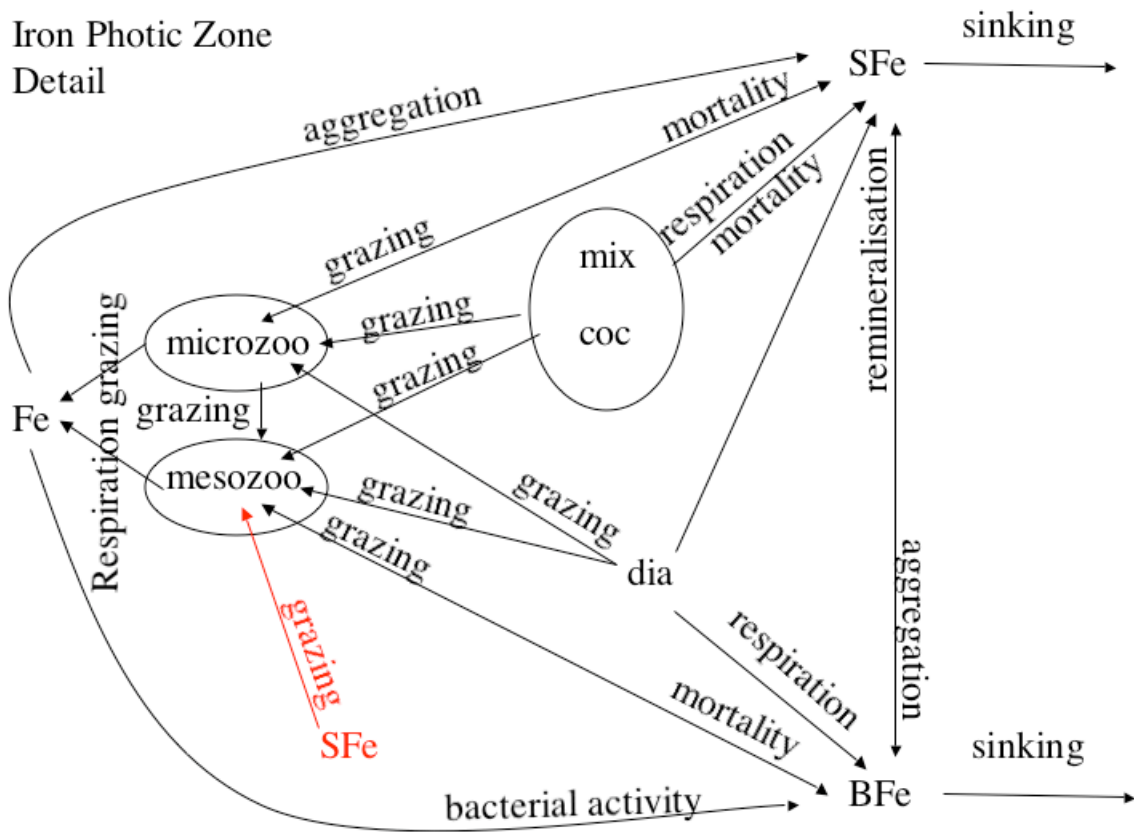


Figure 5. More detailed view of the model iron cycle in the photic zone. SFe = iron in small particulates, BFe = iron in large particulates, mix = mixed phytoplankton, dia = diatoms, coc = coccolithophores, micro = microzooplankton, meso = mesozooplankton.



## Chlorophyll

Chlorophyll content of the three plankton types is explicitly modelled (Fig. 6), but the total chlorophyll content does not have to be conserved (unlike phosphate and silicate). The same and loss processes are present as for phosphate, but modified by the chlorophyll:phosphate ratio. The production terms are also different, resulting in a (slightly) different distribution of chlorophyll compared to the phytoplankton biomass. The chlorophyll concentration is also used to interactively modify the underwater light field, thus modifying the amount of light available for photosynthesis at any given depth.

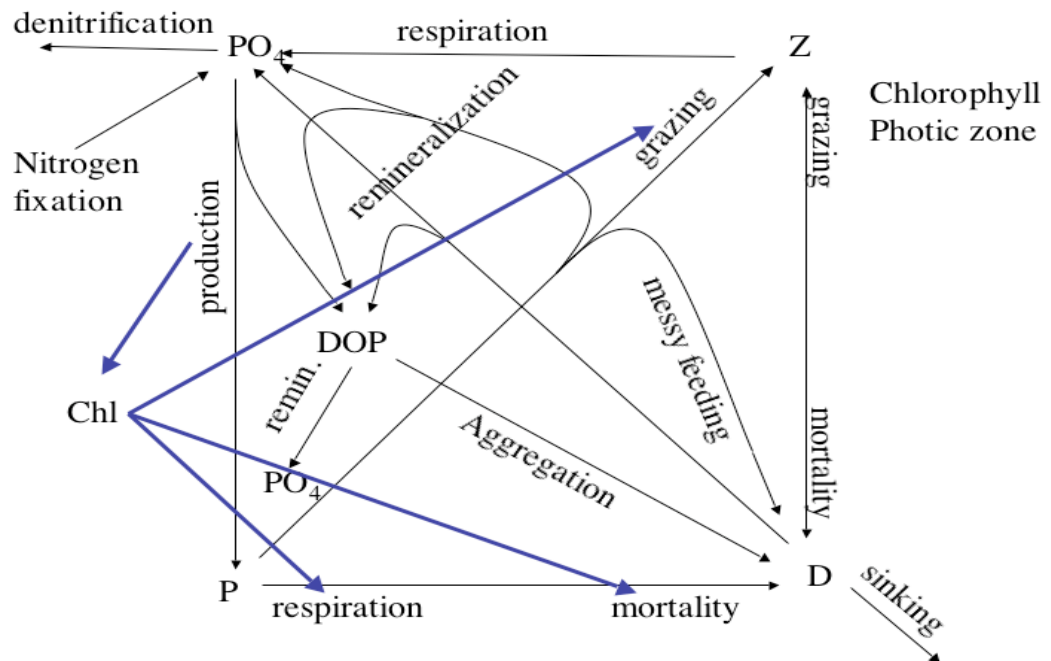


Figure 6. Production and destruction of model chlorophyll (Chl) in the photic zone.

## Calcite and alkalinity

Calcite and alkalinity are both included (Fig. 7).

It will be seen that the calcite and alkalinity cycles are closely connected, the difference being that alkalinity cannot be altered (directly) by air-sea interaction at the surface. Calcite can exist as liths attached to coccolithophores and as detached liths which sink and remineralize to DIC. The production and loss terms are obtained from the equivalent terms for the phosphate equations for coccolithophores, multiplied by a constant factor. DIC is also modified by the processes depicted in Figure 1b, namely phytoplankton production, zooplankton respiration and remineralisation. Similarly alkalinity is also affected by these processes (Figure 7c).

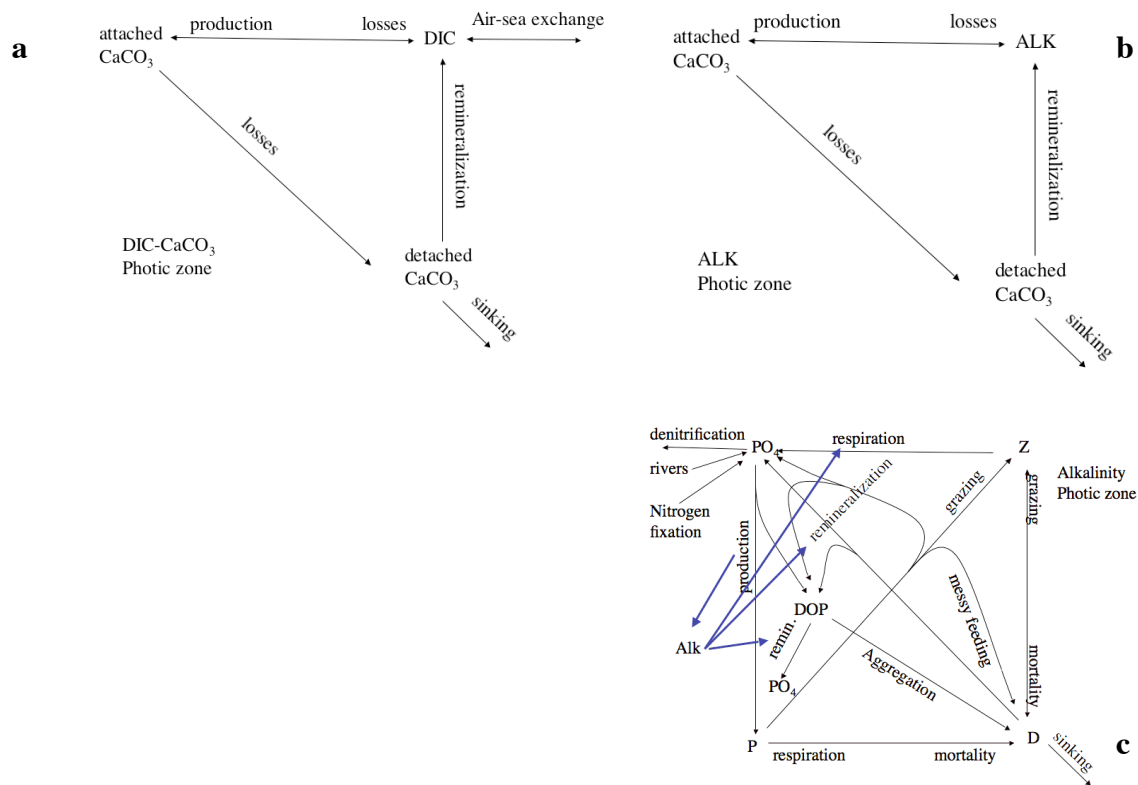


Figure 7. (a) Diagrammatic representation of the model calcite cycle in the photic zone, showing pathways and processes transferring material between Dissolved Inorganic Carbon (DIC), calcite attached to coccolithophores, and detached coccoliths (b) Similar diagram for the model alkalinity (ALK) (c) changes in alkalinity due to production, remineralization and zooplankton respiration.

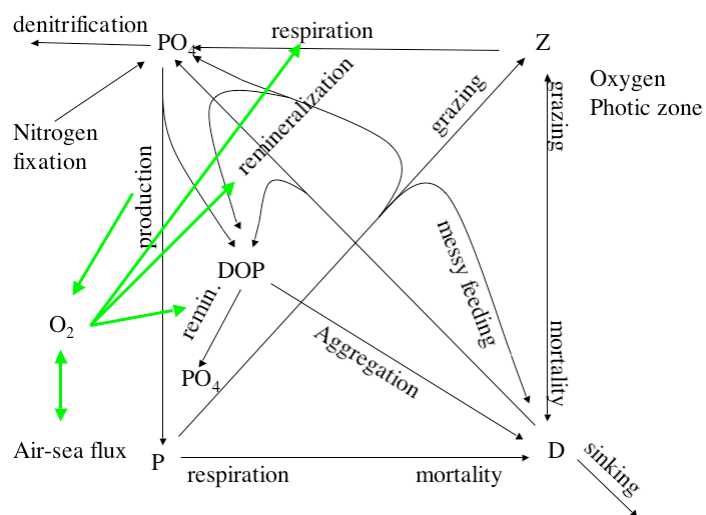


Figure 8. Production and consumption of modelled oxygen in the photic zone.

### Oxygen

Oxygen is consumed by respiration (of zooplankton) and remineralization processes, and produced by photosynthesis (Fig. 8). It can also be modified by air-sea fluxes at the ocean

surface. A by-product of the oxygen cycle is to produce varying amounts of denitrification (removal of phosphate) down the water column. Note that organic material has a fixed oxygen:phosphate ratio of 172:122 in PLANKTOM5.0.

### 3.2 APHOTIC ZONE

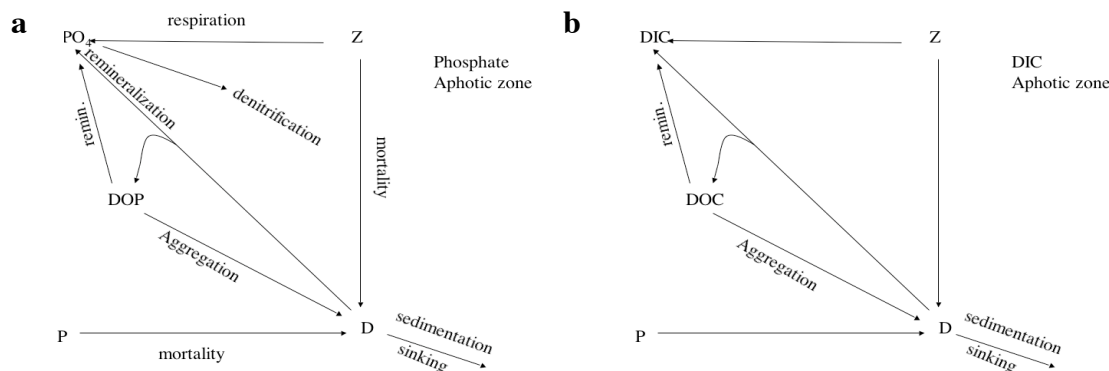


Figure 9. (a) Diagrammatic representation of the model phosphorus cycle in the aphotic zone (b) Similar diagram for the model carbon cycle.

#### Phosphate/carbon cycles

Below the photic zone, the equations are much simpler (Fig 9a, b for phosphate/carbon). Phytoplankton become completely inactive mortality transfers their biomass and nutrients to detritus. Zooplankton continue to respire, but no longer graze. They are subject to mortality which converts them to detritus. Detritus can remineralise (either directly or via DOP/DOC) or sink. DOP/DOC can aggregate to form detritus and as mentioned previously, sedimentation of detritus occurs at the ocean bottom. For completeness, a detailed diagram of the interactions between the various plankton functional types is presented in Figure 10. Since grazing does not occur below the photic zone, the picture is considerably simplified. Most noteworthy is that diatoms are converted to GOC when they die, whereas mixed phytoplankton and coccolithophores are converted to POC.

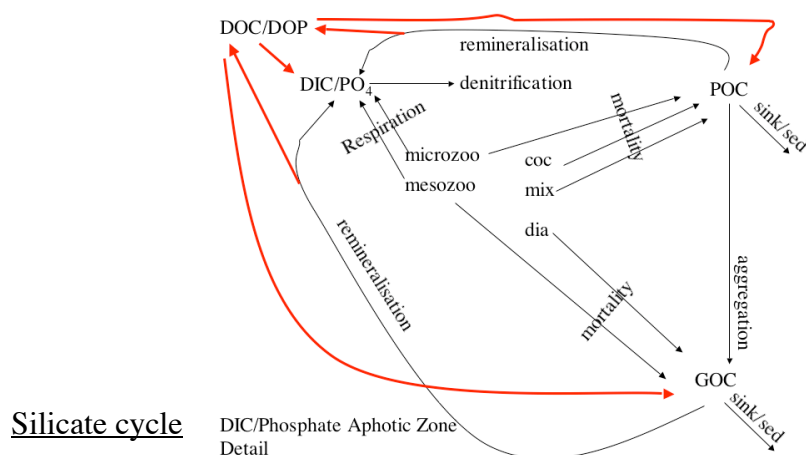


Figure 10. More detailed view of the model phosphorus and carbon cycles in the aphotic zone.

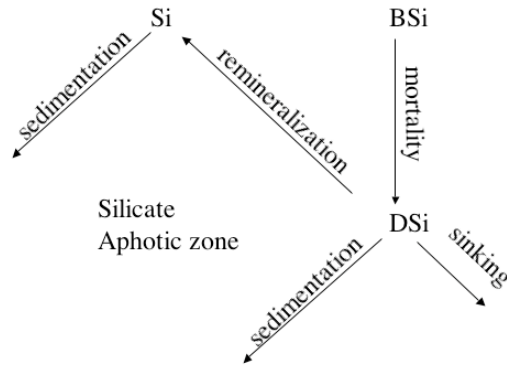


Figure 11. Diagrammatic representation of model silicate cycle in the aphotic zone.

The silicate cycle is also considerably simplified below the photic zone (Fig. 11). Particulate silica is remineralised to dissolved silicate, and mortality transfers silica from diatoms to particulates. Sinking acts to remove particulates at each level and sedimentation occurs at the bottom level. Note that, depending on the relative amounts of particulate and dissolved silicate, either particulates or dissolved silicate are removed by sedimentation at the bottom.

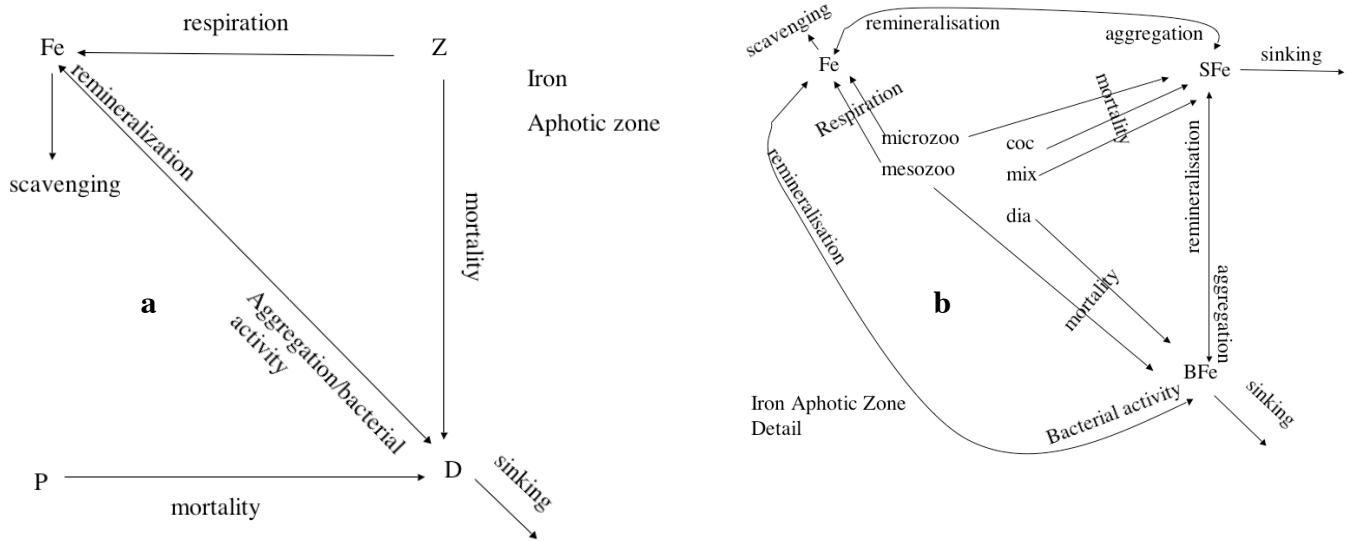


Figure 12. (a) Diagrammatic representation of the model iron cycle in the aphotic zone (b) more detailed view.

### Iron cycle

The pathways for iron in the aphotic zone are summarised in Fig 12 and need no further comment.

### Chlorophyll

Chlorophyll is simply destroyed by mortality in the aphotic zone (Fig. 13).

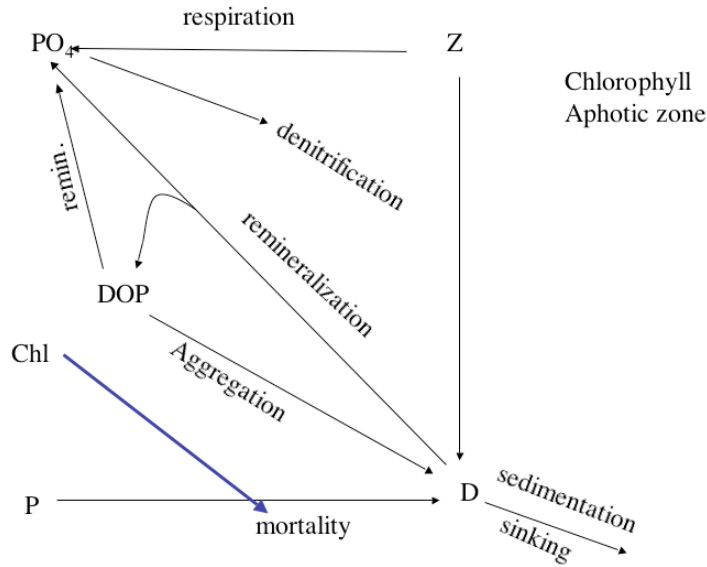


Figure 13. Diagrammatic representation of model chlorophyll in the aphotic zone.

### Calcite and alkalinity

Fig 14 displays the combined diagram for calcite/alkalinity in the aphotic zone. Further loss processes for alkalinity are zooplankton respiration and remineralization. The flows can be inferred from Fig. 9b.

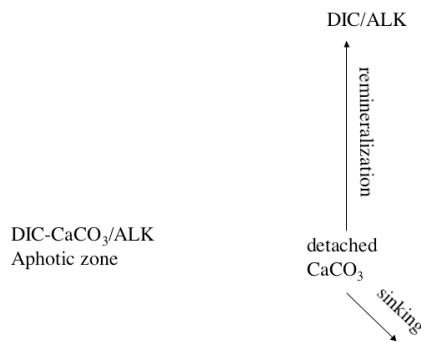


Figure 14. Diagrammatic representation of model calcite/alkalinity cycles in the aphotic zone.

### Oxygen

Below the photic zone, oxygen is consumed by respiration (of zooplankton) and remineralization processes (Fig. 15). Denitrification occurs as a by-product.

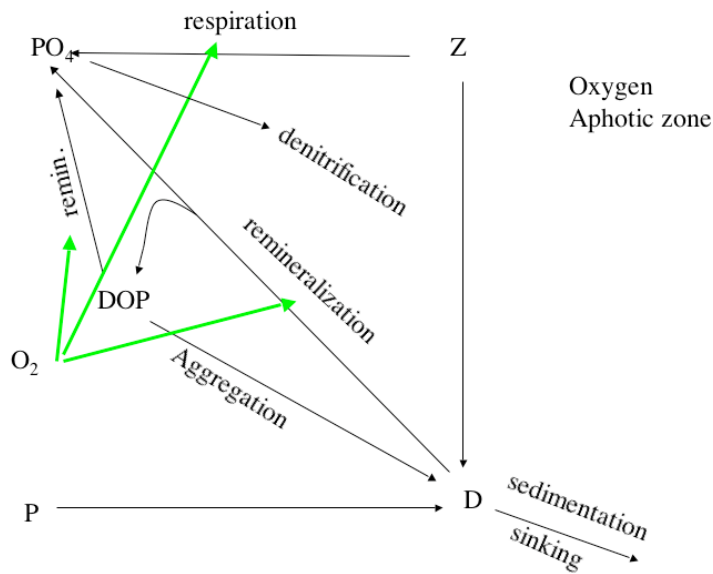


Figure 15. Diagrammatic representation of model oxygen in the aphotic zone.

### 3.3 PARAMETERIZATIONS OF TRANSFER PROCESSES

The processes parameterized in the model are as follows:

- Production
- Light penetration
- Respiration
- Grazing
- Mortality
- Remineralization
- Sinking
- Scavenging of iron
- Aggregation
- Bacterial activity
- Denitrification
- Nitrogen fixation
- Dust and river input
- Sedimentation
- Air-sea fluxes
- Growth efficiency (of zooplankton)

Each process is described briefly below.

## Production

Production terms are computed for carbon/phosphate/silicate, iron, and chlorophyll for each of the three plankton functional types (diatoms, mixed phytoplankton and coccolithophorids). Mixed phytoplankton and coccolithophores are limited by phosphate and iron, diatoms are additionally limited by silicate. Bacteria are limited by phosphate, iron and DOC availability). All the nutrient limitation terms are of the form  $[X]/(K+[X])$  and the lowest value is used to calculate production. The production equations for phosphate/carbon, iron and chlorophyll are slightly different from each other, whereas the production term for silicate is derived from that for phosphate. The light field incident at the surface is attenuated (using an exponential formula) by the depth of water and by the amount of chlorophyll passed through. Red and green wavelengths are treated separately. The photic zone is arbitrarily fixed at about 150m depth or level 18 in OCCAM. Below this level no production occurs.

## Light penetration

The incident PAR is divided equally into two bands corresponding to red and green wavelengths. In the absence of chlorophyll, the light penetration with depth is an exponential function. The absorption coefficient is enhanced when chlorophyll is present in the water column, resulting in shallower penetration.

## Respiration

This is proportional to the square of the concentration for phytoplankton. For zooplankton it is temperature dependent and proportional to the zooplankton concentration.

In the aphotic zone phytoplankton do not respire. Zooplankton continue to respire in the same way as in the photic zone.

## Grazing and zooplankton growth efficiency

Microzooplankton graze on phytoplankton and small detritus (POC), mesozooplankton graze both of these and additionally on large detritus (GOC) and microzooplankton. The grazing rate depends on the concentration of zooplankton multiplied by the concentration of the food, there being a separate term for each food. There is also a coefficient which determines the zooplankton preference for a particular type of food.

Zooplankton growth is fuelled by a proportion of the grazing (total ingestion). This proportion depends (within prescribed limits) on the ratio of zooplankton respiration to total ingestion, the limits being between 0.3 and 0.9 for microzooplankton and between 0.26 and 0.7 for mesozooplankton. The remainder is converted either directly to detritus (“messy feeding”: 10% of the total ingestion) or converted either to nutrient (depends on parameters, currently 0%) or to DOP (currently 90% of the remainder after growth and messy feeding have been accounted for).

The grazing rate for silicate is equal to that for carbon/phosphate multiplied by the ratio of silicate:phosphate in diatoms. All the grazed material is converted to particulates, and none is returned directly to dissolved silicate, neither is any incorporated into zooplankton so the growth efficiency model does not apply.

The growth efficiency model is slightly different for iron compared to phosphate/carbon, inasmuch as there is no dissolved organic phase, and so the remaining iron, after zooplankton growth and transfer to detritus has been accounted for, is returned to the dissolved pool of iron. As alluded to earlier there is also the problem that there may not be sufficient iron in the prey to make up the zooplankton iron:phosphate ratio. When this situation occurs, the growth efficiency is modified so that less phosphate is assimilated and there is thus sufficient iron in the prey to make up the required ratio.

There is no grazing in the aphotic zone.

### Mortality

Phytoplankton are subject to a squared mortality term of the form  $[X]^2/(K+[X])$  in the euphotic zone. The coefficient is modified depending on nutrient availability (phosphate, iron and silicate in the case of diatoms, phosphate and iron in the cases of mixed phytoplankton and coccolithophores). In the aphotic zone the term is similar, but there is no modification due to nutrient availability. Phytoplankton mortality is set to zero if the phytoplankton concentration falls below  $10^{-10}$  mol/L ( $5 \times 10^{-10}$  in the case of diatoms).

Zooplankton mortality is temperature dependent in both photic and aphotic zones and is simply proportional to the zooplankton concentration.

### Remineralization and Sinking

These are treated together in the same subroutine (bgcsnk.F). Detritus is remineralised to DIP/DIC or DOP/DOC and its iron content is remineralized directly to dissolved iron. Particulate silica is remineralized to dissolved silicate and calcite is remineralized to DIC. Only the silicate remineralization is temperature dependent and silicate remineralization only takes place in water depths greater than about 150m or level 18. The remineralization rate is arbitrarily increased to 6/day in the bottom box to prevent accumulation there which can crash the model (this is a modification to allow PLANKTOM5.0 to run in OCCAM).

Two sinking rates are calculated, a slow rate (fixed at 3m/day) for small particles (small POC and small particulate iron) and a faster rate for larger particles (large POC, large particulate iron, particulate silicate and calcite) – this varies with the relative concentrations of calcite, silicate and carbon. The total density of the sinking particles is calculated according to the relative proportions of calcite, silicate and carbon present and the sinking rate varies exponentially with the total density. The sinking rate at each model level is limited to be less than the thickness of the gridbox at that level per leapfrog timestep (2 hours) to prevent numerical instability (another modification for OCCAM).



Sinking and remineralisation occur in the same way throughout both photic and aphotic zones.

#### Scavenging of iron

Scavenging causes iron to be removed from the model (adsorbed onto particulates). The parameterisation is a function of iron concentration as well as POC and GOC. Scavenging occurs in both photic and aphotic zones

#### Aggregation

POC can aggregate to form GOC (and SFE can aggregate to form BFE). The parameterisation consists of a term in the square of POC concentration and another in the product of POC and GOC concentrations. Two other terms are also functions of vertical diffusivity (turbulence). The sum of these four terms is the aggregation term. For iron aggregation the terms are multiplied by the ratio of iron:carbon in the detritus. Aggregation of DOC to POC or GOC is dealt with below. DOC contains no iron so is not a source of SFE or BFE. However dissolved iron can aggregate to form small particulates and bacterial activity can transfer iron from the dissolved state to large particulates (see below). Aggregation occurs throughout the water column in the same way.

#### Bacterial activity

Bacterial activity contributes to two processes to the model: uptake of iron; and aggregation of DOC into small and large particulates. Bacterial activity is limited by DOC, iron and phosphate, with limitation terms similar to those for phytoplankton production.

#### Denitrification

As mentioned earlier, the production and loss terms in the phosphate equation, are used to determine the generation and consumption of oxygen (by multiplying by the ratio of oxygen:phosphorus = 172:122 in organic material). All the production is used to generate oxygen (and to fix phosphate). However some of the oxygen consumption is used to fuel denitrification (parameterised as loss of phosphate). In other words, the loss terms are driven by a combination of oxygen and phosphate, the proportions being decided by the ambient oxygen concentration. If the oxygen concentration is high, little denitrification takes place, if it is low, a lot of denitrification takes place and therefore oxygen is not depleted further.

#### Nitrogen fixation

The volume integrated denitrification for the whole model is calculated at each timestep and the amount of nitrogen fixation at the surface is adjusted to balance this quantity. However rather than adding a constant amount at each surface gridbox, the nitrogen fixation is allowed to vary horizontally depending on the potential for nitrogen fixation at each location. The actual fixation is of phosphate of course since the model doesn't explicitly model the nitrogen cycle.

## Dust and river input

Dust input at the surface is converted into source terms for silicate and iron equations. The input files are monthly means, and the model interpolates linearly to give a value at each timestep and at each gridpoint. Fig. 16 shows the annual mean dust input on the OCCAM grid.

River input is read in as DIC and DOC. The silicate input by rivers is derived from DIC and the phosphate input from DIC+DOC. The source terms in the equations are thus fixed values at specified coastal gridpoints, passed on the annual mean DIC and DOC input at those gridpoints. Figure 17 shows the distribution and magnitude of the river input terms on the OCCAM grid.

Iron input is also specified at coastal points. In this case no input data is read in, but a mask of all the coastal points is read in. At these gridpoints, extra source terms are included for dissolved iron down to depth level 8 (exponentially diminishing with depth). Deeper coastal points have no extra iron input for levels 9 to just above the seabed. However the seabed gridpoint does have the extra term. PLANKTOM-OPA includes about half a dozen extra deep sea points where coastal iron is released to account for submerged or unresolved islands (e.g. Kerguelan Island). These are not included in the PLANKTOM-OCCAM model.

## Sedimentation

In order to conserve the total amount of phosphate and silicate which are subject to dust and river input a special subroutine removes an equivalent amount of tracer from the seabed gridboxes. For silicate, each gridbox loses a proportion of the global input of silicate from dust and rivers as either loss of dissolved silicate, or loss of particulate silica (the model prefers to remove dissolved silicate, unless insufficient is available at that gridpoint, in which case it removes particulate silica). Scaling is applied to the loss terms to ensure global conservation of silicate.

For phosphate a similar procedure is applied, although the loss terms are removed from POC and GOC, which would seem to violate carbon conservation.

Iron input at coastal points is not removed at the bottom, and as noted before there is no requirement for iron conservation in PLANKTOM5.0.

## Air-sea fluxes

Fluxes of CO<sub>2</sub> and O<sub>2</sub> at the ocean surface are computed from DIC and oxygen fields in combination with surface windspeed, humidity, atmospheric O<sub>2</sub> and CO<sub>2</sub> concentration, sea-surface temperature and sea-ice cover which are supplied by the physical model forcing.

### **3.4 Changes introduced to the PLANKTOM5.0 code**

#### Code organisation

There are eleven subroutines associated with PLANKTOM5.0. They are called in turn by OCCAM's biological subroutine, biosource.F. The latter is called as the model deals with

each tracer gridpoint in subroutine tracer.F. The names of the subroutines and a summary of their functions is given below:

bgcprg.F – sets constants, fills river input arrays and calls other subroutines.  
bgcche.F – sets chemical constants.  
bgcint.F – performs time interpolation of dust and other data where required.  
bgclys.F – treats dissolution of CaCO<sub>3</sub>.  
bgcbio.F – computes biological trends in the photic zone.  
bgcpro.F- applies light field and calculates production.  
bgclos.F – calculates loss terms.  
bgcsnk.F – calculates sinking and remineralisation terms.  
bgcnul.F – protect against negative values.  
bgcrem.F - computes biological trends in the aphotic zone.  
bgcsed.F – computes sedimentation and nitrogen fixation.  
bgcflx.F – calculates air-sea fluxes of CO<sub>2</sub> and O<sub>2</sub>.

Associated .h (include) files are as follows:

common.passivetr.c.dgom.h  
common.passivetr.h  
parameter.passivetr.c.dgom.h  
parameter.passivetr.h  
trclsm.dgom.h

Changes to each subroutine

#### bgcprg.F

Sets river input data. The bulk of the PLANKTOM5.0 parameters are now initialized here rather than being read in from a namelist. River input (cotdep and po4dep) are set to zero for the run described here.

#### bgcche.F

The first time bgcche is called, the array hi (H<sup>+</sup> concentration) is initialized.  
kgwanin = is set to 0.31\*ws\*ws (no chemical enhancement of O<sub>2</sub> fluxes).

#### bgcint.F

No changes.

#### bgclys.F

Remineralisation rates of calcite (remco3) set to 1/2 on sea-bottom gridbox. Remco3 is prevented from becoming negative elsewhere in the water column. This subroutine was formulated in terms of tendencies of DIC, calcite and alkalinity, now formulated in terms of actual tracer values – therefore additional factor of rfact included.

### bgcbio.F

Bug fix - prodt in bgcbio has one line in the wrong position.

Plankton, POC and GOC fields cannot fall below  $1 \times 10^{-10}$  for the purposes of tendency calculations, previously set to zero if less than  $1 \times 10^{-8}$

SFE and BFE cannot fall below  $1 \times 10^{-13}$  for the purposes of tendency calculations previously no restriction.

DFE, NFE, CFE cannot fall below  $1 \times 10^{-13}$  for the purposes of tendency calculations previously no restriction.

ensure delno3 cannot drag  $\text{PO}_4$  below zero.

Volume averaged diagnostics of each term in the phosphate, iron and silicate cycles can be turned on or off with -D flags.

Special treatment of sinking term on sea-bottom gridbox as jk+1 may cause a problem.

Sets dust input data

### bgcpro.F

Chlorophyll cannot go below  $1 \times 10^{-11}$  for the purposes of primary production calculation - previously it could go down to  $5 \times 10^{-10}$

Carbon content of plankton cannot go below  $1 \times 10^{-10}$  for the purposes of primary production calculation - previously no restriction.

Iron content of plankton cannot go below  $1 \times 10^{-13}$  for the purposes of primary production calculation - previously no restriction.

Minimum value of zero for production terms prophy. and limitation terms xlimpft and xlimbac

Silicate limitation term xlim3 in bgcpro was becoming large and negative - for mixed phytoplankton and cocolithophores. Had to alter code, xlim3 only applied to diatoms.

Ensure limitation terms (xlimpft, xlimdoc and xlimbac) are larger than zero.

Ensure phosphate/carbon, iron, chlorophyll, and silicate production terms (prophy, prorca3) do not fall below zero.

Light field from daily cloud cover (on the OPA model grid) supplied by Erik Buitenhuis (currently residing as .nc files in /scratch/azo1/bablu/erik\_cloud\_data).

Used program readncclouds3.f to do the calculation then Andrew Yool used Matlab to interpolate to OCCAM grids and create daily .txt files.

### bgclos.F

Plankton, POC and GOC fields cannot fall below  $1 \times 10^{-8}$  for the purposes of tendency calculations, previously set to zero if less than  $1 \times 10^{-8}$ .

SFE and BFE cannot fall below  $1 \times 10^{-13}$  for the purposes of tendency calculations previously no restriction.

DFE, NFE, CFE cannot fall below  $1 \times 10^{-13}$  for the purposes of tendency calculations previously no restriction.

BSI cannot fall below  $1 \times 10^{-10}$  for the purposes of tendency calculations previously no restriction.

Chlorophyll fields cannot fall below  $1 \times 10^{-11}$  for the purposes of tendency calculations, previously no restriction.

Following tendency terms are prevented from falling below zero: resphy, torphy, resps, torts, grazm, grazz, grazpoc, grazgoc, gramic, grames, grazss, grazs.

Micrge is set to fall between rn\_ggemc and 1.-rn\_unamic.

Mesoge is set to fall between rn\_ggemes and 1.-rn\_unames.

#### bgcsnk.F

Sinking rates have max value of  $0.9 \times \text{gridbox thickness}$  per timestep (2 hours) except in layer 1 where the minimum is 4.5m per timestep.

Minimum value of zero for remik, remip, xbactfer, xagg, xaggdfe, xaggdoc, xaggdoc2, siremin, xscave and xaggfe.

Minimum value of  $3 \times 10^{-10}$  for phymoy

Remineralisation rates of olimi, orem, orem2, osil, ofer, ofer2 are set to 1/2 on sea-bottom gridbox.

Remineralization rates are prevented from becoming negative.

Sinking rates are prevented from becoming negative.

#### bgcnul.F

Minimum value for variables = ccbio =  $1 \times 10^{-11}$  except for iron and chlorophyll related variables where it is  $1 \times 10^{-14}$ .

Explicit fix for calcite - sinking rates set to zero if concentration goes negative.

Special treatment of sinking terms on sea-bottom gridbox as jk+1 may cause a problem.

No protection introduced for silicate and DOC, they can in theory go negative in the euphotic zone.

Bug in original code: rn\_sigmes\*respz2(jk) should be respz2(jk).

Special fix for euler timesteps implemented (this is an OCCAM specific requirement).

#### bgcrem.F

Zooplankton fields cannot fall below  $1 \times 10^{-10}$  for the purposes of tendency calculations, previously set to zero if less than  $1 \times 10^{-9}$ .

Zooplankton, chlorophyll, iron, POC, GOC, DOC, DSI, SFE and BFE protected from going below zero (strictly  $1 \times 10^{-11}$  or  $1 \times 10^{-14}$  for iron related variables) in bgcrem – otherwise causes all sorts of problems including crashing the model.

Ensure delno3 cannot drag  $\text{PO}_4$  below zero.

Special treatment of sinking terms on sea-bottom gridbox as jk+1 may cause a problem.

Calcite, oxygen and silicate can in theory go negative below the euphotic zone because they aren't protected.

#### bgcsed.F

Calculates integrals of DSI, silicate and POC+GOC for sea-bottom boxes to be summed by master processor.

Calculates integrals of denitrification and potential nitrogen fixation throughout water column for sea-bottom boxes to be summed by master processor.

Uses summed values from last timestep sent by master processor to weight sedimentation and nitrogen fixation terms to ensure (near) conservation.

#### bgcflx.F

qcumul commented out. This subroutine was formulated in terms of tendencies of DIC and oxygen, now formulated in terms of actual tracer values – therefore additional factor of rfact included.

### **4. Experimental set up and input files**

This is similar to that described in SY06. The main differences are in the initialisation and forcing of the biological tracers.

#### Light Field

The biological equations of the model are forced with a different light field to the physical equations. This may seem odd, but was necessary to ensure a fair comparison between PLANKTOM-OCCAM and PLANKTOM-OPA, since the latter uses daily averaged irradiance with no diurnal cycle. Accordingly, the irradiance for the biological equations was calculated offline using exactly the same procedure as the OPA model, using as input daily cloud cover (on the OPA model grid) supplied by Erik Buitenhuis (currently residing as .nc files in /scratch/azo1/bablu/erik\_cloud\_data). One netcdf file, containing cloud cover, air temperature, humidity, windspeed and precipitation, was supplied for each day between 1985 and 2005. A FORTRAN program (readncclouds3.f) was used to perform calculation of daily mean surface irradiance for each day. The results for each day were stored in separate ascii files. These ascii files were then interpolated to the OCCAM grids using Matlab and output as daily ascii files. For example there are two files for 8 May 1989: bs.may89.08.occam\_g1.sw and bs.may89.08.occam\_g2.sw corresponding to OCCAM model grids 1 (145x360 values) and 2 (111x111 values). The procedure to read these in to the model is described in Section 2 (item 3).

#### Dust and river input

The dust input files are generated from data supplied by Erik Buitenhuis in a similar way to the cloud cover files described in the previous section, except that there are far fewer files and they only need to be read in once at the beginning of a run. The dust data was received as one netcdf file containing one variable for each of 12 months on the OPA grid. This was read into Matlab and interpolated to the OCCAM grids. The interpolated data was output to 24 ascii files (dust\_jan1.txt, dust\_jan2.txt etc). These files are quite small and as there are only 24 of them, they are placed in the run directory (e.g. /noc/omf/working/oikos/bs/coapec1/OCCAM/run157) for each run. The procedure for reading them into the model at runtime is detailed in Section 2 (item 2). The spatial distribution of the dust data is shown in Fig. 16.

The river data is treated slightly differently. The river data also comes in one netcdf file containing DIC and DOC on the OPA grid. These were read in to FERRET and output as ascii files. The ascii files were then read in by a FORTRAN program which stripped out the zero values leaving only the river inputs on the coastal points and their latitudes and longitudes (980 gridpoints in total). These were read in by another FORTRAN program which also read in the latitudes and longitudes of the OCCAM grids. The nearest OCCAM gridpoint was selected for each OPA gridpoint, and the river data was assigned to this OCCAM gridpoint, hence the 980 OPA gridpoints were assigned to 980 equivalent OCCAM gridpoints. Full 2D arrays for DIC and DOC were then written out in a similar format as for the dust files (rdic1.txt, rdic2.txt, rdoc1.txt and rdoc2.txt). These were also placed in the run directory. The procedure for reading them into the model at runtime is detailed in Section 2 (item 2). The geographical distribution of the river data is shown in Fig. 17.

Finally iron is deposited at coastal points (down to level 8) and at the sea-bed gridpoints. The coastal points were found using a FORTRAN program (cmask3.f), and a coastal mask was created for the OCCAM grid with the value 1 at coastal points and zero elsewhere. The mask was written in ascii format to files cmask31.txt and cmask32.txt and placed in the run directory. The procedure for reading them into the model at runtime is detailed in Section 2 (item 2).

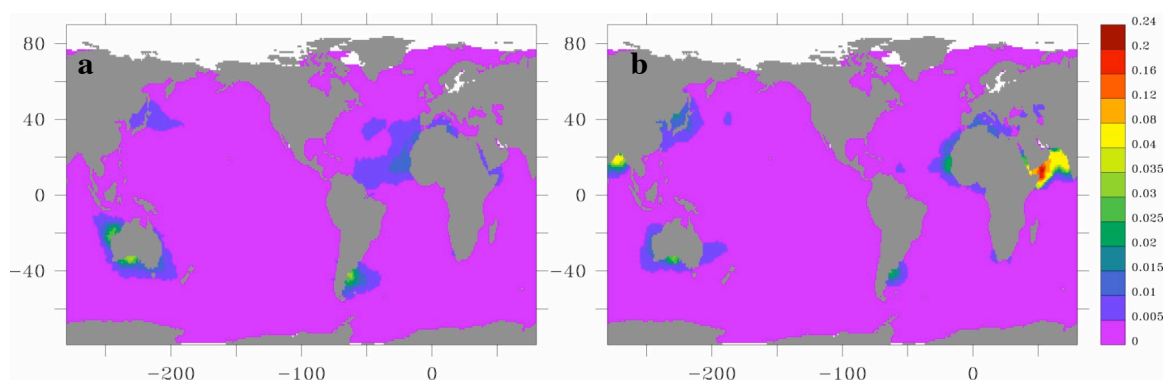


Figure 16. Monthly mean dust input files ( $\text{g m}^{-2} \text{ month}^{-1}$ ) (a) January, (b) July

### Restart files

Generation of initial restart files was dealt with by YS06 (Section 4, pp15-20). The procedure followed here is essentially the same except that it was decided to initialize the model with an interpolated version of the restart file for 31<sup>st</sup> December 1988 used by the PLANKTOM-OPA simulation. The interpolation procedure was carried out in directory /noc/omf/scratch/marquest/erik\_initial\_restart\_1989.

The PLANKTOM-OPA restart file (obtained from Erik Buitenhuis) is called restart\_19881231\_trc.nc. The data for biogeochemical fields is first converted to ascii format using FERRET (listdgom.script), and then regridded to the OCCAM grids (using script runregrid\_dgom which executes FORTRAN programs regrid\_dgom1b.f/regrid\_dgom2b.f). The resulting ascii data files are then converted to binary format using script

runconvert\_dgom\_vars (which runs FORTRAN programs regrid\_dgom1b.f/regrid\_dgom2b.f). The binary data created is then combined with existing physics variables from an OCCAM physics-only simulation (z2924.restart/z2924.restart2 – see Popova et al., 2006a) using FORTRAN programs create\_dgom\_restart1a.F/create\_dgom\_restart2a.F. The new restart files are named z9999.restart1 and z9999.restart2 and can be renamed as desired (see Section 7 of SY06) and a new run started. The physical model is initialised at the beginning of 1981 and run for 8 years as described in Popova et al. (2006). The physical fields thus obtained for December 31 1988 are merged with the initial biogeochemical fields to create a restart file for PLANKTOM-OCCAM as described above. The physical model is forced with NCEP/NCAR Reanalysis data (Kalnay et al., 1996) as modified by Large and Yeager (2004). See also Coward and de Cuevas (2005) for more details. In brief, the surface windstress and the surface sensible and latent heat are calculated from meteorological variables air temperature, humidity, surface air temperature, atmospheric pressure and surface winds specified at 6-hourly intervals. Downward longwave and shortwave radiation are specified at daily intervals and snow and precipitation are specified at monthly intervals. A diurnal cycle is imposed on the incident shortwave radiation (for physics only, not biogeochemistry as explained previously). There is also a weak relaxation on the surface salinity to prevent model drift.

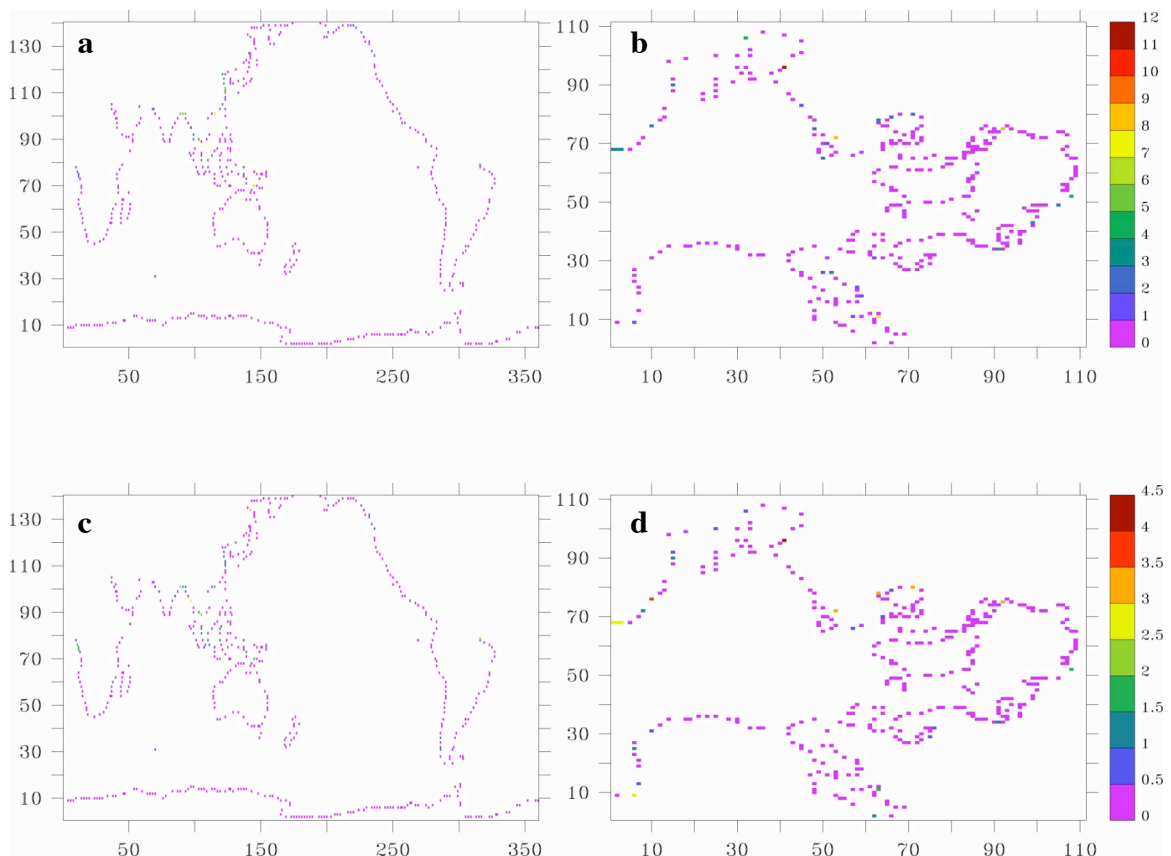
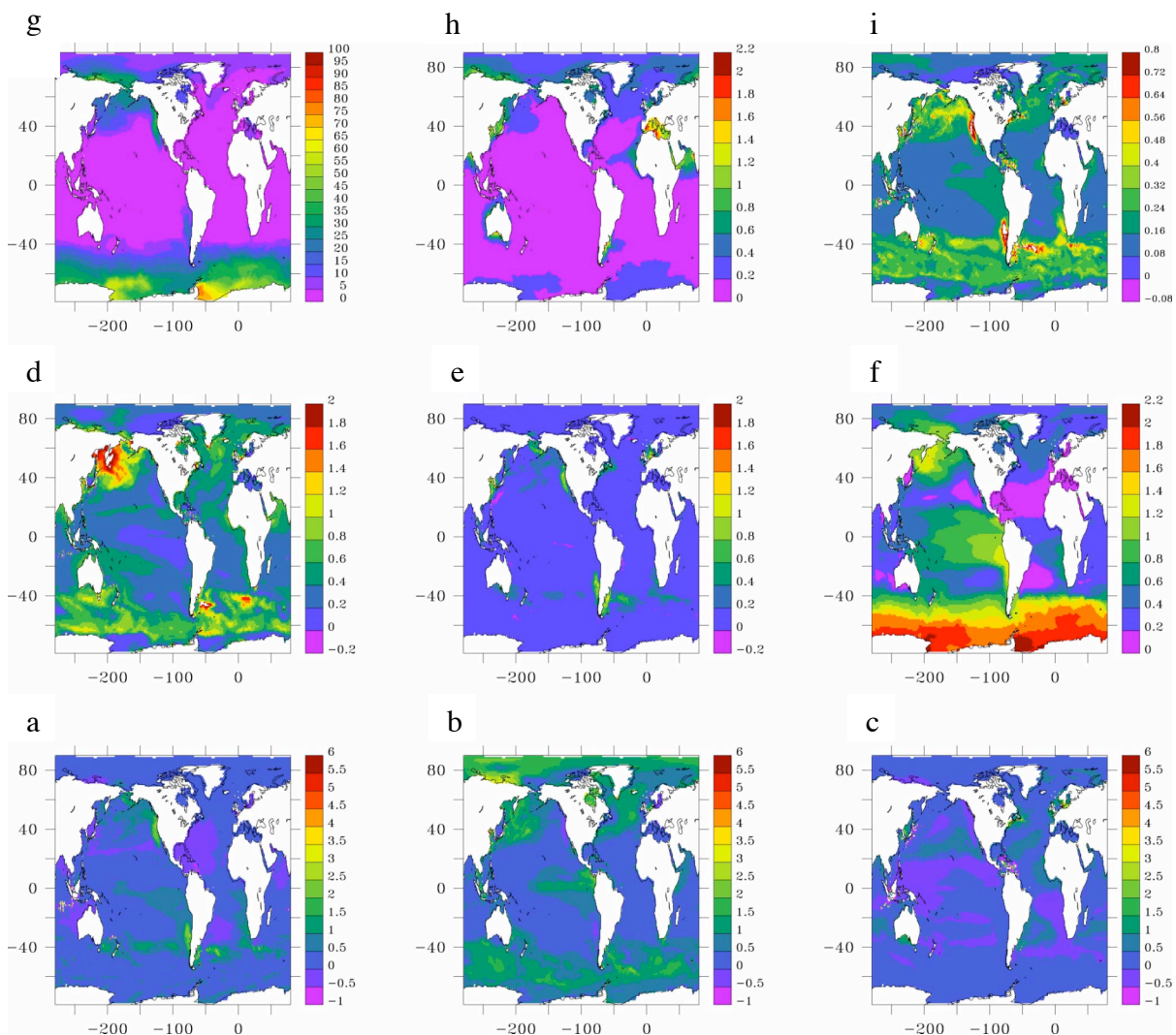


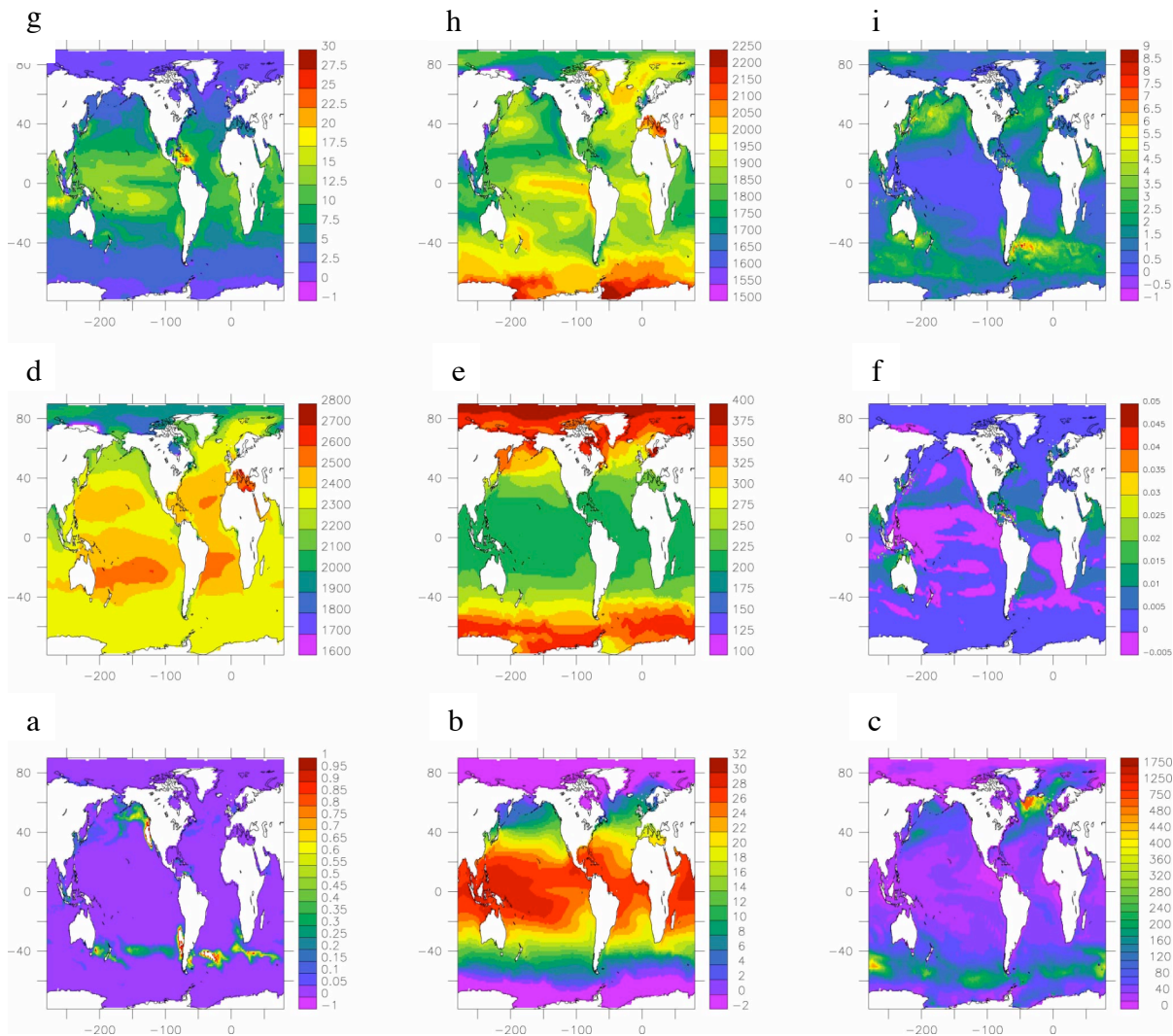
Figure 17. Annual mean river input files ( $\text{Tg yr}^{-1}$  per model box) (a) DIC, OCCAM grid 1 (b) DIC, OCCAM grid 2 (c) DOC, OCCAM grid 1, (d) DOC, OCCAM grid2. Axes labels denote model gridpoint indices.



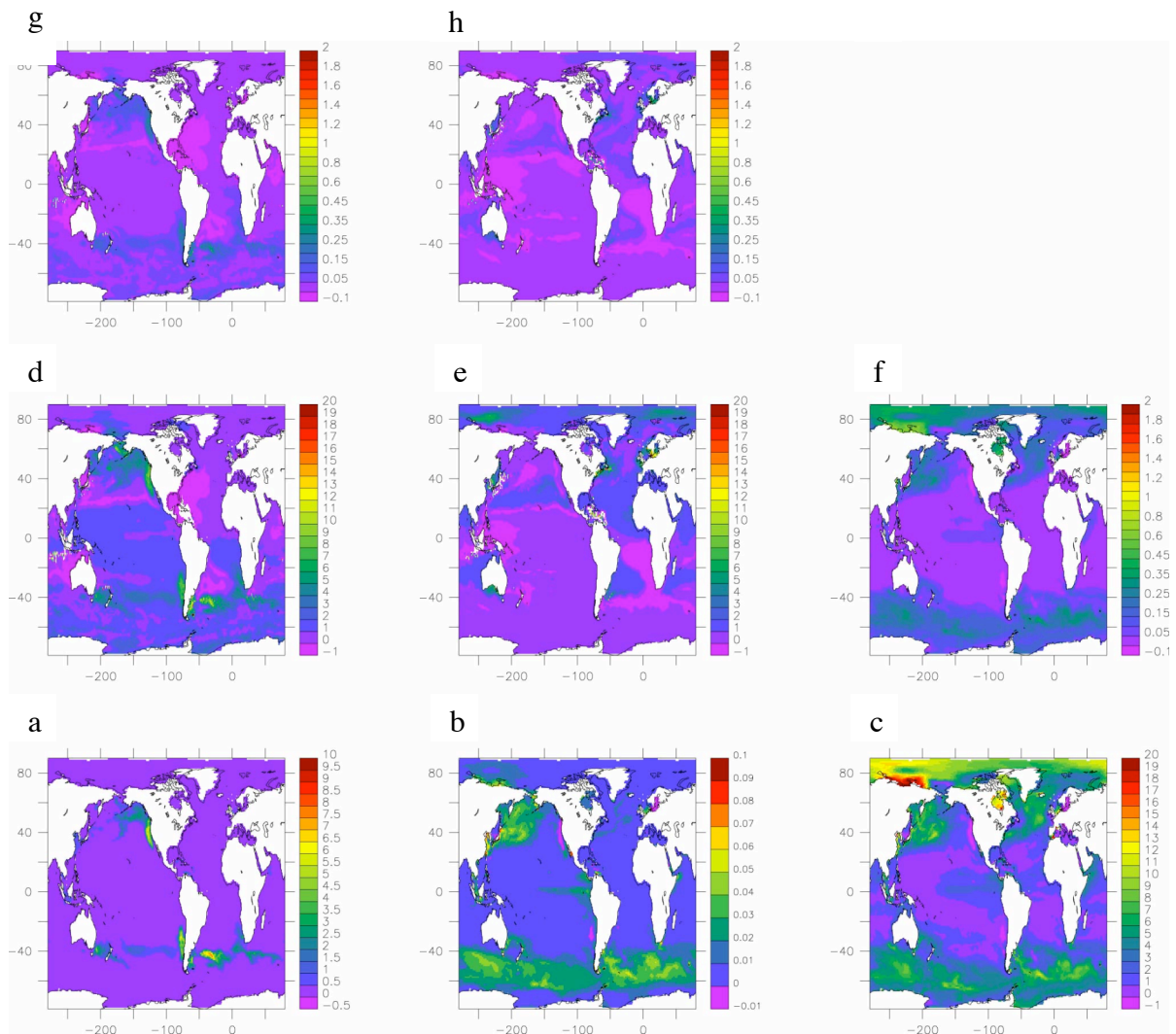
For the purposes of this report we simply display annual mean surface distributions of the PLANKTOM5.0 biogeochemical tracer fields. A more detailed analysis will be performed in a later publication. Fig 18. Displays annual mean surface concentrations of the plankton functional types, the three nutrients, and POC for year 1994 of the PLANKTOM-OCCAM simulation. Figure 19 shows GOC, surface temperature, mean daily maximum mixed layer depth, alkalinity, oxygen, calcite, DOC, DIC and SFE. Figure 20 shows BFE, DSI, and iron and chlorophyll content of diatoms, mixed phytoplankton and coccolithophores. At the time of writing BSI was not available to be plotted.



18. Annual mean surface fields from year 1994 of the PLANKTOM-OCCAM simulation (a) mixed phytoplankton (b) diatoms (c) coccolithophores (d) microzooplankton (e) mesozooplankton (f) phosphate (g) silicate (h) iron (i) POC. Plankton fields and POC are in  $\text{mmol C m}^{-3}$ . Phosphate is in  $\text{mmol PO}_4 \text{ m}^{-3}$ , Silicate is in  $\text{mmol SiO}_3 \text{ m}^{-3}$ , iron is in  $\mu\text{mol Fe m}^{-3}$ .



19. Annual mean surface fields from year 1994 of the PLANKTOM-OCCAM simulation (a) GOC in  $\text{mmol C m}^{-3}$  (b) sea-surface temperature in  $^{\circ}\text{C}$  (c) mean daily maximum mixed layer depth in m (d) alkalinity in  $\text{mmol m}^{-3}$  (e) oxygen in  $\text{mmol m}^{-3}$  (f) calcite in  $\text{mmol m}^{-3}$  (g) DOC in  $\text{mmol C m}^{-3}$  (h) DIC in  $\text{mmol C m}^{-3}$  (i) SFE in  $\text{nmol Fe m}^{-3}$ .



20. Annual mean surface fields from year 1994 of the PLANKTOM-OCCAM simulation (a) BFE (b) DSI (c) DFE (d) NFE (e) CFE (f) DCH (g) NCH (h) CCH. Iron fields are in  $\text{nmol Fe m}^{-3}$ . Chlorophyll fields are in  $\text{mg m}^{-3}$ . DSI is in  $\text{mmol m}^{-3}$ .

## 6. Acknowledgements

We wish to thank Andrew Yool (NOC) for performing interpolation of dust input data. We thank Erik Buitenhuis (University of East Anglia) for supplying the PLANKTOM5.0 code, dust and river input files and atmospheric boundary layer forcing data (including cloud cover). We also thank him for assistance in implementing PLANKTOM5.0 in OCCAM.

## 7. References

- Coward, A. C., and de Cuevas, B. A., 2005, The OCCAM 66 Level Model: physics, initial conditions and external forcing. *Southampton Oceanography Centre Internal Report No. 99*, 58pp (unpublished manuscript).
- Kalnay, E., et al., 1996, The NCEP/NCAR 40-year reanalysis project. *Bull. Amer. Meteor. Soc.*, 77, 437-471.
- Large, W. G., Danabasoglu, G., and Doney, S. C., 1997, Sensitivity to surface forcing and boundary layer mixing in a global ocean model: annual –mean climatology. *J. Phys. Oceanogr.*, 27, 2418-2446.
- Large, W. G., and Yeager, S. G., 2004, Diurnal to decadal global forcing for ocean and sea-ice models: the datasets and flux climatologies, *NCAR Technical Note*, NCAR/TN-460+STR, 104pp.
- Le Quéré, C., Harrison, S. P., Prentice, I. C., Buitenhuis, E. T., Aumont, O., Bopp, L., Claustre, H., Cotrim Da Cunha, L., Geider, R., Giraud, X., Klaas, C., Kohfeld, K. E., Legendre, L., Manizza, M., Platt, T., Rivkin, R. B., Sathyendranath, S., Uitz, J., Watson, A., J., and Wolf-Gladrow, D., 2005, Ecosystem dynamics based on plankton functional types for global ocean biogeochemistry models. *Global Change Biology* 11, 2016-2040.
- Marsh, R., de Cuevas, B. A., Coward, A. C., Bryden, H. L., and Alvarez, M., 2005, Thermohaline circulation at three key sections of the North Atlantic over 1985-2002. *Geophys. Res. Lett.*, 32, L10604, doi:10.1029/2004GL022281.
- Marsh, R., Josey, S. A., Nurser, A. J. G., de Cuevas, B. A., and Coward, A. C., 2005, Water Mass Transformation in the North Atlantic over 1985-2002 simulated in an eddy permitting model. *Ocean Science*, 2, 1-18.
- Popova, E. E., Coward, A. C., Nurser, G. A., de Cuevas, B. A., Fasham, M. J. R., and T. R. Anderson, 2006, Mechanisms controlling primary and new production in a global ecosystem model – Part I: Validation of the biological simulation. *Ocean. Sci.*, 2, 249-266.
- Popova, E. E., Coward, A. C., Nurser, G. A., de Cuevas, B. A., and T. R. Anderson, 2006, Mechanisms controlling primary and new production in a global ecosystem model – Part I:

The role of the upper ocean short –term periodic and episodic mixing events. *Ocean. Sci.*, 2, 267-279.

Sinha, B. and A. Yool, 2006, Extension of the OCCAM 1 ocean general circulation model to include the biogeochemical cycles of carbon and oxygen PART I: Technical Description, *National Oceanography Centre Southampton Research and Consultancy Report No. 6*, 81pp.

Yool, A., and B. Sinha, 2006, Extension of the OCCAM 1 ocean general circulation model to include the biogeochemical cycles of carbon and oxygen PART II: Technical Description, *National Oceanography Centre Southampton Research and Consultancy Report No. 5*, 159pp.